JOURNAL OF CATALYSIS 129, 145–158 (1991)

# Platinum/Zeolite Catalyst for Reforming *n*-Hexane: Kinetic and Mechanistic Considerations

GERALD S. LANE,[1] FRANK S. MODICA, AND JEFFREY T. MILLER

*Amoco Oil Company, P.O. Box 3011, Naperville, Illinois 60566*

Received July 9, 1990; revised December 5, 1990

A platinum/L-zeolite-reforming catalyst exhibits higher activity and selectivity for converting *n*-hexane into benzene than other Pt catalyst. The reaction pathways indicate that for all catalysts, e.g., Pt/K L or Pt/K Y, benzene is formed as a primary product by one–six-ring closure and methylcyclopentane is formed as a primary product via one–five-ring closure. The ratio for one–six to one–five-ring closure, however, is about two times greater for the Pt/K L than for the Pt/K Y, or other platinum catalysts. The preference for the one–six-ring closure in L zeolite appears to be related to the optimum pore size of the L zeolite. In addition to an increased selectivity for one–six-ring closure, the Pt/K L-zeolite catalyst also displays increased reactivity. For example, the turnover frequency of the Pt/K L-zeolite catalyst is 10 times higher for formation of benzene and 3.3 times higher for formation of methylcyclopentane compared with the Pt/K Y-zeolite catalyst. Although the Pt/K L is more reactive than Pt/K Y, the apparent activation energies, 54 kcal/mol for one–six-ring closure and 39 kcal/mol for one–five-ring closure, are the same for both catalysts. Differences in reactivity are associated with an increase in the preexponential term for the Pt/K L catalyst. The increased aromatics selectivity for Pt/K L is consistent with the confinement model which proposes that *n*-hexane is adsorbed as a six-ring pseudo-cycle resembling the transition state for one–six-ring closure. 

## INTRODUCTION

In petroleum refining, the demand for increased octane and decreased light-end products stimulates the need for finding alternative ways to convert light, $C_6$–$C_8$, paraffins into aromatics with high yields. In conventional reforming, many of the $C_6$–$C_8$ paraffins hydrocrack over the acidic platinum/alumina or platinum–rhenium/alumina catalysts, rather than cyclize to aromatics. Recent reports (*1–5*) demonstrate an alternative, more selective reforming catalyst, platinum supported on nonacidic L zeolite. The nonacidic, L-zeolite reforming catalyst differs from conventional, bifunctional reforming catalysts (platinum on chlorided alumina) in that it is monofunctional, having only a metal (platinum) function. The L-zeolite catalyst, therefore, benefits from the absence of acid-catalyzed hydrocracking resulting in higher liquid yields. Monofunctional reforming catalysts form aromatic products via one–six-ring closure and are unable to directly convert methylcyclopentane into benzene (Fig. 1). Among the nonacidic zeolite catalysts, platinum supported on L zeolite exhibits the best activity and selectivity (*5*). Several explanations have been proposed to explain the increased selectivity of Pt/L-zeolite catalyst. Two explanations relate the improved selectivity to the geometry of the zeolite support (6–8). Alternatively, the basicity of the support and related influences of cations on the electronic state (electron density) of platinum have also been proposed to account for selectivity improvements of Pt/K L catalyst (*9*). One explanation (*6, 7*), the molecular die hypothesis, proposes that the channels of the zeolite orient the diffusing hexane molecules with their long axes parallel to

[1] To whom correspondence should be addressed.



0021-9517/91 $3.00

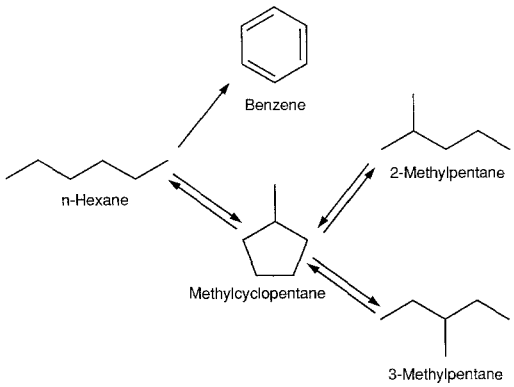


FIG. 1. Reaction pathway for monofunctional reforming catalysts using *n*-hexane as the reactant.

the L-zeolite channel. This leads to terminal adsorption of the hexane molecule with the platinum, which is speculated to increase the selectivity for one–six-ring closure. The second geometric explanation (*8*), the confinement (conformation) model, suggests that adsorption of *n*-hexane in the zeolite pores leads to preorganization of *n*-hexane as a pseudo-cycle resembling the transition state for ring closure. Based on molecular modeling, the L-zeolite geometry is suggested to be the proper size for preorganization of *n*-hexane for one–six-ring closure. The preorganization of the transition state would lower the free energy of activation of the transition state by enthalpic and/or entropic effects. For platinum in Y zeolite, geometric effects have also been reported, and selectivity for methylcyclopentane ring opening is dependent on the size of the platinum cluster relative to the size of the zeolite pore (*10*). These effects might also be expected to affect the one–six-ring closure selectivity in zeolite catalysts. However, none of the previous proposals accounts for the increased activity of the Pt/L-zeolite catalyst.

In an attempt to develop some understanding of the novel performance of the platinum/L-zeolite catalyst, a study of the reactions of *n*-hexane at atmospheric pressure was undertaken to compare platinum supported on potassium-exchanged L and Y zeolites. The reaction pathways and apparent kinetic parameters were compared for the Pt/K L and Pt/K Y catalysts. In addition, the activities and selectivities for cyclization, e.g., formation of benzene and methylcyclopentane, over platinum supported on alkalized alumina, Na Y zeolite, and silica were compared.

## EXPERIMENTAL

### *Catalyst Preparation*

Catalysts were prepared from nonacidic supports by impregnating a platinum salt, decomposing the platinum salt, and by reducing the platinum. The nonacidic supports were obtained as commercial samples or were synthesized. Sodium Y (LZY-52, 10.30 wt% Al and 9.60 wt% Na) and potassium L (ELZ-L, 11.75 wt% Al and 7.73 wt% K) zeolites were commercial samples obtained from Union Carbide. Potassium Y zeolite (10.20 wt% Al, 2.73 wt% Na, and 9.30 wt% K) was obtained by ion exchange (five exchanges with 0.15 *M* $KNO_3$) of the commercial Na Y zeolite. The silica (Cab-O-Sil, HS-5) was obtained from Cabot Corporation. Boehmite, alumina sol (90% $H_2O$ and 10% $Al_2O_3$), free of sodium and sulfate salts, was obtained from Criterion (formerly American Cyanamid). Five percent potassium nitrate, on a dry weight basis of $Al_2O_3$ (1.9% K), was dissolved into the $Al_2O_3$ sol. Alkalized $\gamma$-alumina was obtained by precipitation of the boehmite with excess $NH_4OH$, followed by drying and calcination at 550°C for 16 h. The supports are referred to as silica, K $Al_2O_3$, Na Y zeolite, K Y zeolite, and K L zeolite. To each support, platinum was impregnated using an aqueous solution of tetraammineplatinum(II) nitrate to weight loadings of 1.0% platinum. The platinum-impregnated catalysts were calcined for 3 h in air at 260°C, and then reduced in hydrogen (50 ml/min) at 500°C for 1 h.

*Characterization*

Transmission electron microscopy (TEM) and CO chemisorption were used to characterize the location and size of the platinum particles and to estimate the available platinum surface area, respectively. The electron microscope was a Phillips 400T TEM operated at 120 kV and equipped with a Tracor Northern 550 energy-dispersive X-ray spectrometer. The TEM samples were prereduced, ground to a fine powder, embedded in LR white resin, and sectioned with an ultramicrotome. The thin sections were mounted on copper grids and lightly coated with carbon. The CO chemisorption capacity of each catalyst was measured at 25 ± 3°C by the dynamic-pulse-flow technique after *in situ* reduction (*11*).

*Catalyst Testing*

An atmospheric-pressure, bench-scale apparatus provided a simple means of evaluating catalytic performance using a fixed-bed, continuous-flow reactor. The reactor consisted of a 0.8-cm-i.d. quartz tube with an internal thermocouple. The experiments were conducted using between 10 and 400 mg of catalyst combined with $\alpha$-alumina to give a total loading of 0.6 g. Both the catalyst and the $\alpha$-alumina were screened to 20/45-mesh granules and were supported on a bed of quartz wool. The reactor was operated under flowing hydrogen, and *n*-hexane (Aldrich, 99.6+% purity) was added by saturation of hydrogen through a bubbler at room temperature. In all experiments, the $H_2$/HC molar feed ratio was kept constant at 7.8. Prior to any experiment, the catalyst was reduced *in situ* at 500°C in flowing hydrogen (50 ml/min) for 1 h. Temperature effects were studied by varying the temperature from 330 to 440°C while holding the *n*-hexane feed rate constant at 1.4 g/h and feeding 50 ml/min $H_2$. Alternatively, the effect of space velocity (*n*-hexane conversion) on product selectivity was studied at a constant temperature of 420°C by changing the mass of catalyst and/or changing the flow rate of the *n*-hexane–hydrogen feed mixture. Reproducible results with minimal effects from deactivation were determined by waiting for the temperature and flow rates to stabilize and then starting the hydrogen flow through the bubbler; after waiting an additional 5 min, the product was sampled. After the data were obtained at all desired space velocities, the temperature was returned to the original setting to determine the extent of deactivation. No deactivation was observed for the Pt/K L and Pt/K Y catalysts over the temperature range examined. Product analyses were conducted by off-line gas chromatography using a 30 m × 0.53 mm, RSL-160 bonded capillary column. Control experiments using only the $\alpha$-alumina packing showed no measurable conversion.

## RESULTS

*Transmission Electron Microscopy*

TEM images the zeolite surfaces and provides visual comparisons of the platinum particle sizes. Figures 2 and 3 illustrate representative micrographs of the Pt/K Y and Pt/K L catalysts, respectively. Figure 2a shows the Y zeolite is made up of angular particles ranging in size from 0.3 to 1 $\mu$m. Lattice images of the Y zeolite show spacings of 1.44 nm and are observed in several regions of Fig. 2b. The visible platinum is present in 1.0 to 2.0 nm particles and is distributed uniformly throughout the Y zeolite. Electron micrographs at higher magnifications (not shown) show the platinum particles bridging two adjacent zeolite cages. A micrograph of the L-zeolite catalyst (Fig. 3a) shows the L-zeolite particles to be rounded or rectangular in shape, ranging in size from 0.03 to 0.5 $\mu$m. Lattice images, with spacings of 1.66 nm, are shown to be normal to the channel direction in the rectangular particles, whereas the rounded particles show the zeolite lattice looking down the channel direction. In three-dimensional space, the L-zeolite particles appear to be

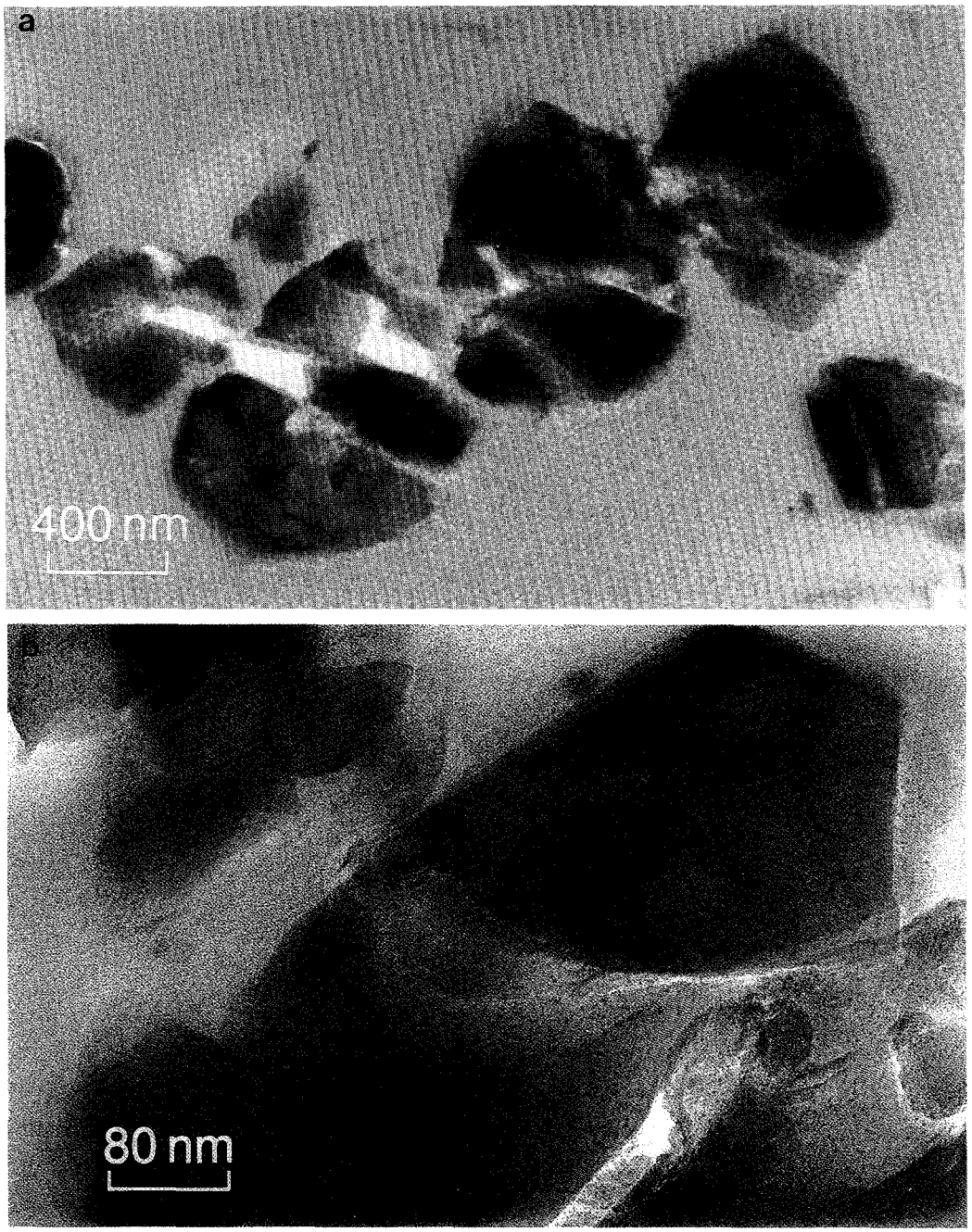


FIG. 2. Representative electron micrographs of the Pt/K Y-zeolite catalyst. The dark spots of catalyst 2b are platinum particles.

cylindrical in shape with the unidirectional channels parallel to the cylindrical axis. Most of the platinum particles are too small to be observed even at $10^6\times$ magnification. The platinum that is observed in Fig. 3b appears to be uniformly dispersed with particle sizes less than 1.0 nm.

In general, the electron microscopy re-

sults suggest the L-zeolite crystallites are smaller than the Y zeolite by about an order of magnitude. In addition, the platinum particles are smaller in size for the L-zeolite catalyst, with most of the platinum particles too small to be resolved by the microscope. Both catalysts are shown to have very highly dispersed platinum located inside the zeolite channels, with the largest platinum particles being on the order of 2.0 nm.

*Catalyst Performance*

Platinum catalyzes a variety of different reactions, and many of these reactions have been used to probe the nature of platinum in a variety of catalysts. On the supports used in this study, the main reactions (at low conversion) were conversion of *n*-hexane to benzene by one–six-ring closure and to methylcyclopentane by one–five-ring closure. Small amounts of $C_5^-$ products (methane, ethane, etc.) result from hydrogenolysis on the platinum. Conversion is defined as the amount of *n*-hexane converted to other products based on weight percent.

*Reaction profiles.* The reaction profiles for the catalysts were compared by varying the weight hourly space velocity (WHSV) at a constant temperature. Figures 4 and 5 show the reaction profiles at 420°C as a function of *n*-hexane conversion for the Pt/K L and Pt/K Y catalysts, respectively. Note that Figs. 4 and 5 are plotted with different scales on the ordinate axes and that the benzene mole percent has been plotted against the right ordinate axis in Fig. 4b. Both catalysts show the same general trends: methylcyclopentane exhibits a maximum between 40 and 60% conversion, 2-methylpentane and 3-methylpentane exhibit maxima around 80% conversion, and $C_5^-$ products and benzene increase with *n*-hexane conversion. The other catalysts, Pt/Na Y zeolite, Pt/K $Al_2O_3$, and Pt/$SiO_2$, exhibit the same reaction profiles (not shown) as the Pt/K L and Pt/K Y catalysts.

An analysis of the reaction pathway involves discriminating between primary and nonprimary products. Traditionally, this analysis is performed by plotting concentration of a given product versus the inverse space velocity. In this method, a positive initial slope indicates a primary product, and a zero slope indicates a nonprimary product. Often, the extrapolation of concentration to zero contact time (infinite space velocity) fails to provide a clear indication if the initial slope of a given curve is zero or nonzero. An alternative method has been developed (*12*) which provides another means of determining the reaction network and the order of appearance of products. Primary products are determined by plotting component selectivities as a function of reactant conversion and extrapolating to zero conversion. If the intercept is zero, the product is nonprimary, and if the intercept is nonzero the product is primary. Secondary products can be determined by plotting (component selectivity)/(conversion) as a function of reactant conversion. In this case, primary products diverge at zero conversion (they have infinite intercepts); secondary products have finite intercepts, and higher-order products have zero intercepts. A detailed description and proof of this method can be found elsewhere (*12*).

Applying this technique to the results obtained when reacting *n*-hexane over the nonacidic catalysts discriminates the major primary products from the nonprimary products. Figures 6a and 6b show the application of this technique to the reaction products for the Pt/K L-zeolite catalyst at 420°C. In Fig. 6, selectivity is defined in mole percent. A plot of component selectivities as a function of *n*-hexane conversion, Fig. 6a, shows benzene and methylcyclopentane are, predominantly, primary products with nonzero intercepts, and the hexane isomers (2-methylpentane and 3-methylpentane) and $C_5^-$ products have small intercepts. Component selectivity/conversion plotted as a function of *n*-hexane conversion, Fig. 6b, illustrates that 2-methylpentane, 3-methylpentane, and $C_5^-$ products have finite, nonzero intercepts, while benzene and methylcyclopentane diverge at low conversion.

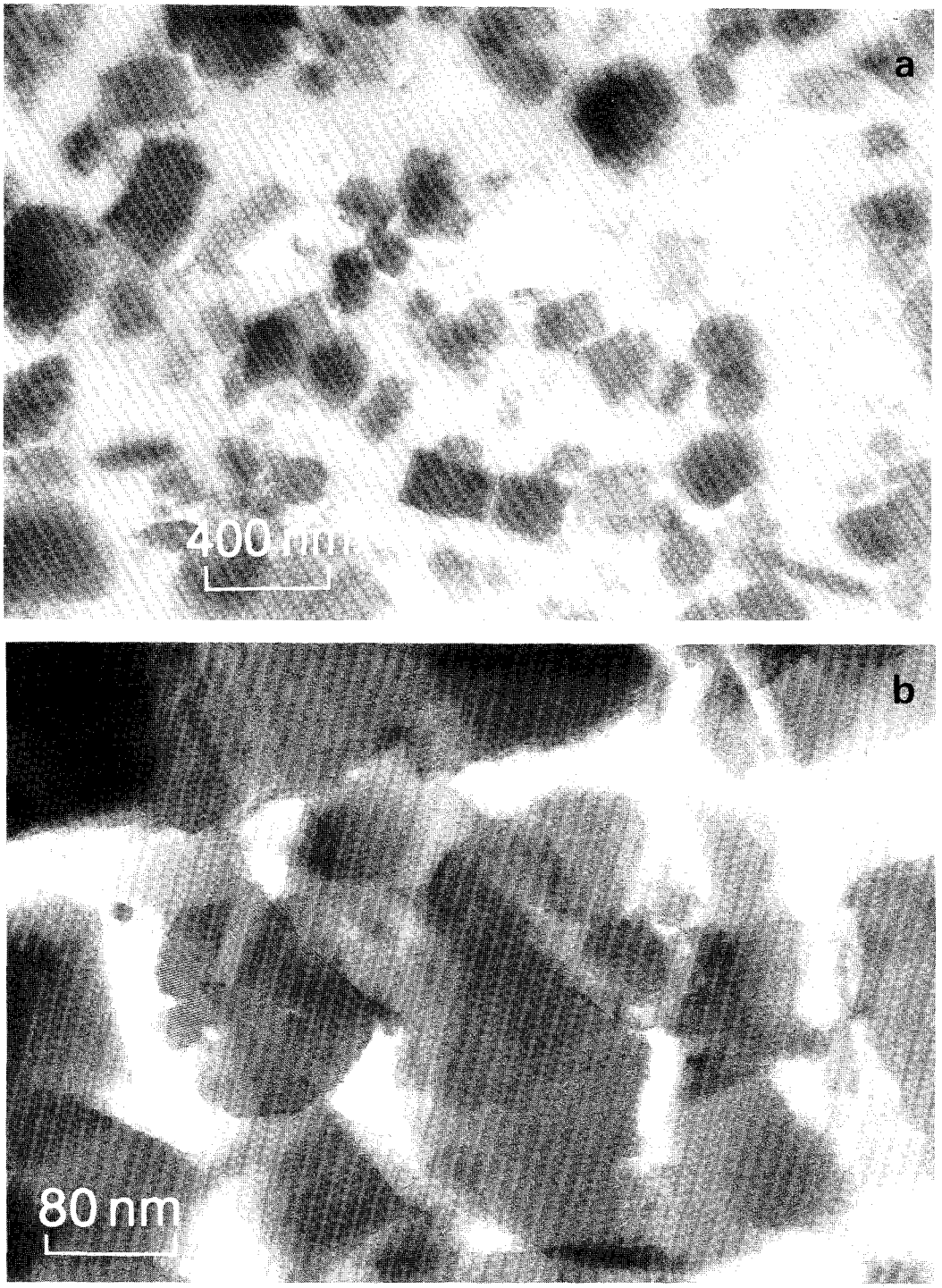


FIG. 3. Representative electron micrographs of the Pt/K L-zeolite catalyst.

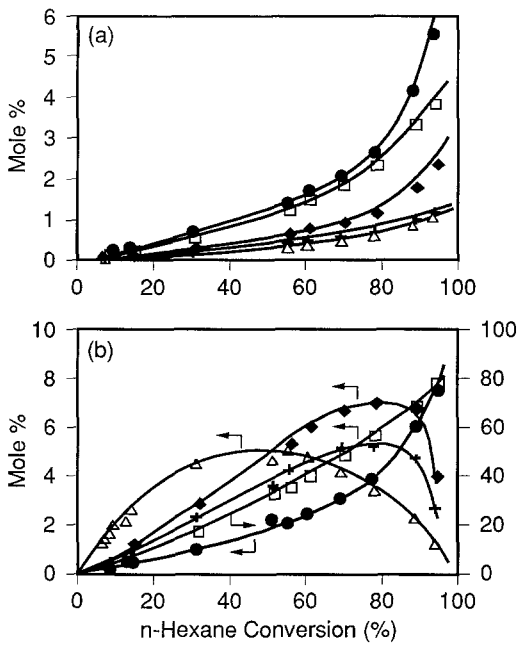


FIG. 4. Reaction profile as a function of *n*-hexane conversion (wt%) for the Pt/K L catalyst at 420°C in mole percent. (Note scale change for benzene.) (a) ● methane, ♦ ethane, + propane, △ butanes, and □ pentanes; (b) ● $C_1$–$C_5$, △ methylcyclopentane, ◆ 2-methylpentane, + 3-methylpentane, and □ benzene.

Methylcyclopentane, observed to be a primary product in Fig. 6a, goes through a maximum in Fig. 4, indicating that it is converted to secondary products. At high conversion in Fig. 4, the yields of 2-methylpentane and 3-methylpentane begin to decline, indicating that reverse reactions are becoming important. All this suggests that the reaction profile illustrated in Fig. 1 is a plausible network for the conversion of *n*-hexane on the Pt/K L catalyst.

The reaction profiles for the other catalyst were also analyzed using this technique. Generally, the results were the same as those depicted in Figs. 6a and 6b. For the five catalysts tested, methylcyclopentane and benzene were determined to be the major primary products; 2-methylpentane and 3-methylpentane were determined to be predominantly secondary products. For all catalysts except $Pt/SiO_2$, the yield of $C_5^-$ products, including propane, was low. For $Pt/SiO_2$, propane was determined to be a primary product, likely due to acidic hydrocracking of *n*-hexane by the $SiO_2$ support.

*Selectivity*

For the purposes of evaluating these catalysts, the following definitions are used to describe the selectivities of the catalysts. Benzene selectivity is the amount of *n*-hexane converted to benzene divided by the total amount of *n*-hexane converted (in weight percent). Since hexane isomers (methylcyclopentane, 2-methylpentane, and 3-methylpentane) can back react to form benzene as shown in Fig. 1, a second benzene selectivity has been defined to reflect the losses to $C_5^-$ products when converting all $C_6$ paraffins to benzene. This second selectivity, referred to as the ultimate benzene selectivity, is the amount of hex-

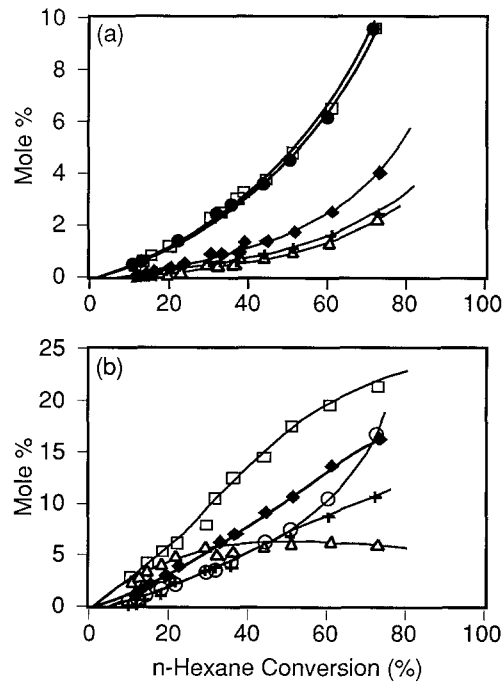


FIG. 5. Reaction profile as a function of *n*-hexane conversion (wt%) for the Pt/K Y catalyst at 420°C in mole percent. (a) ● methane, ♦ ethane, + propane, △ butanes, and □ pentanes; (b) ● $C_1$–$C_5$, △ methylcyclopentane, ♦ 2-methylpentane, + 3-methylpentane, and □ benzene.

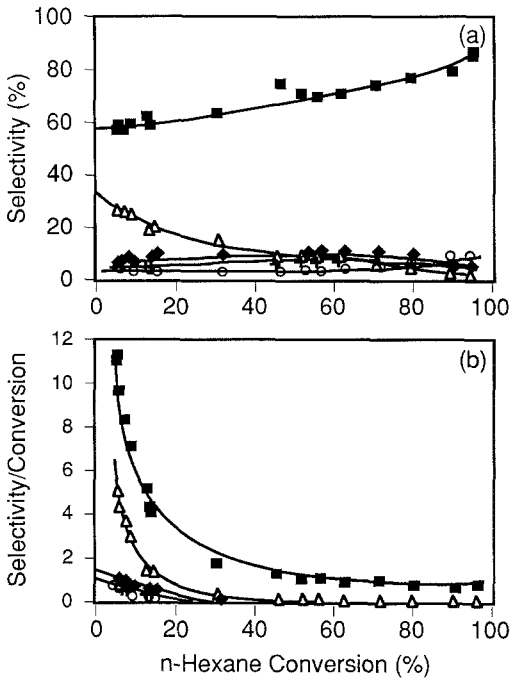


FIG. 6. Primary and secondary product discrimination for Pt/K L (a) component selectivity as a function of reactant conversion (nonzero intercepts indicate primary products), and (b) component selectivity/conversion as a function of reactant conversion (nonzero, convergent intercepts indicate secondary products). ● $C_1$–$C_5$, △ methylcyclopentane, ◆ 2-methylpentane, + 3-methylpentane, and □ benzene.

anes converted to benzene divided by the amount of hexanes converted to benzene and to light, $C_1$–$C_5$, hydrocarbon products (in weight percent). Also, at the temperatures used in this study, ring opening of methylcyclopentane occurs at a rate faster than that of ring closure; therefore, even at low conversions, 2-methylpentane and 3-methylpentane were always observed along with methylcyclopentane. The selectivity for ring opening of methylcyclopentane is defined as the mole ratio of 2-methylpentane to 3-methylpentane.

Table 1 summarizes the benzene selectivities of the catalysts at low *n*-hexane conversion. The benzene selectivities demonstrate the selectivity advantage for the Pt/K L-zeolite catalyst. For example, the Pt/K L-zeolite catalyst exhibits a benzene selectivity of 0.57 compared to a benzene selectivity of 0.32 for the Pt/K Y-zeolite catalyst. The benzene selectivity, as defined previously, penalized catalysts that exhibit high isomerization rates, because the isomerized products (methylcyclopentane, 2-methylpentane, and 3-methylpentane) are considered by-products. However, the reaction pathway, Fig. 1, shows that these isomerized products can back react to form benzene. In other words, *n*-hexane, methylcyclopentane, 2-methylpentane, and 3-methylpentane are not considered as products but are considered as reactants to form either benzene or light hydrocarbon gases. To account for this effect, Table 1 summarizes the ultimate benzene selectivity of each catalyst, i.e., benzene selectivity at 100% $C_6$ paraffin conversion. The Pt/K L-zeolite catalyst shows a remarkable ability to form benzene with an ultimate benzene selectivity of 0.93. The Pt/K Y-zeolite catalyst, by comparison, exhibits an ultimate benzene selectivity of only 0.73. With the exception of the $Pt/SiO_2$, which had some weak support acidity evidenced by the formation of propane, i.e., hydrocracking, the other catalysts demonstrate ultimate benzene selectivities greater than 0.70.

TABLE 1

Catalyst Selectivities at 420°C

| Catalyst[a] | Benzene selectivity[b] | Ultimate benzene selectivity[c] | Ring opening MCP 2-MP/3-MP[d] |
|---|---|---|---|
| Pt/K L | 0.57 | 0.93 | 1.8 |
| Pt/K Y | 0.32 | 0.73 | 2.0 |
| Pt/Na Y | 0.32 | 0.87 | 2.0 |
| $Pt/K\text{-}Al_2O_3$ | 0.25 | 0.73 | 2.0 |
| $Pt/SiO_2$ | 0.18 | 0.55 | 1.7 |

[a] Each catalyst contains 1.0 wt% Pt.

[b] Benzene selectivity—the fraction of *n*-hexane converted to benzene to *n*-hexane converted to other hydrocarbon products in weight percentage.

[c] Ultimate benzene selectivity—the fraction of hexanes converted to benzene to hexanes converted to benzene and light, $C_1$–$C_5$, hydrocarbon products in weight percentage.

[d] Relative formation of 2-methylpentane to 3-methylpentane from the ring opening of methylcyclopentane, which was formed during the conversion of *n*-hexane extrapolated to 0% *n*-hexane conversion.

Thus, whether compared on the basis of the benzene selectivity or ultimate benzene selectivity, the Pt/K L-zeolite catalyst offers significant selectivity advantages over the other catalysts.

As shown in Fig. 1, the two dominant reaction paths for *n*-hexane are one–six-ring closure to form benzene and one–five-ring closure to form methylcyclopentane. In Table 1 the benzene selectivity is seen to be *dependent* on the catalyst support showing a large increase in benzene selectivity for the Pt/K L-zeolite catalyst compared to the other catalysts.

Although the catalysts show selectivity differences for aromatization of *n*-hexane, the selectivity for the ring opening of methylcyclopentane is essentially independent of the catalyst. Table 1 summarizes the 2-methylpentane/3-methylpentane ratios observed for all catalysts extrapolated to zero conversion. For all five catalysts this ratio is near 2.0. Even at high conversions, the selectivity for ring opening is essentially *independent* of the catalyst support. Thus, the catalysts support affects the benzene selectivity, but does not affect the selectivity for ring opening of methylcyclopentane.

*Relative activity.* A previous report (*5*) demonstrates the activity of the Pt/L-zeolite catalyst for cyclizing light paraffins to aromatics exceeds that of other platinum catalysts. Figure 7 shows the superior performance of the Pt/K L-zeolite catalyst at 420°C. For example, at 2 WHSV (0.5 1/WHSV), the Pt/K L-zeolite catalyst has converted nearly 90% of the *n*-hexane, whereas the best of the other catalysts (Pt/K Y-zeolite catalyst) has converted only 50%. Assuming the reaction is first order in *n*-hexane, the slope of each line in Fig. 7 represents the rate constant for a given catalyst at low conversions. Taking the ratio of the slopes of two lines, over the differential conversion range, provides a measure of the relative activities on a per gram of catalyst basis. This is equivalent to determining the space velocity required by a given catalyst to attain a set conversion divided by the

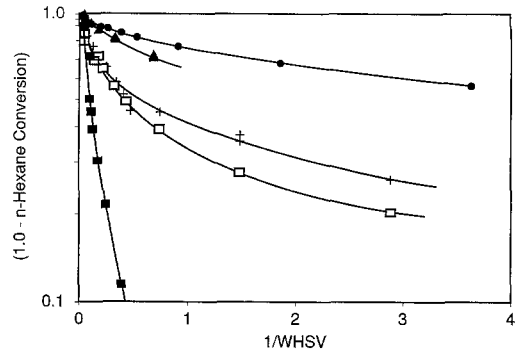


FIG. 7. Comparison of catalyst activities per gram of catalyst for a series of catalysts: ■ Pt/K L, □ Pt/K Y, + Pt/Na Y, ▲ Pt/K $Al_2O_3$, and ● Pt/$SiO_2$. Conditions are 420°C and a molar feed ratio of $H_2$/*n*-hexane of 7.8.

space velocity required by the reference catalyst to attain the same conversion. Designating the Pt/K L-zeolite catalyst as the reference, the relative activities per gram of catalyst were calculated at 10% *n*-hexane conversion. Table 2 summarizes the relative activities for each catalyst in Fig. 7. The Pt/K L-zeolite catalyst (relative activity = 100) exhibits more than five times the activity of the Pt/K Y-zeolite catalyst (relative activity = 18). The Pt/Na Y-zeolite catalyst has nearly the same relative activity, 16, as the Pt/K Y-zeolite catalyst, while the Pt/$Al_2O_3$ and Pt/$SiO_2$ exhibit relative activities of 5 and 3, respectively.

*Turnover frequencies.* From a commercial application standpoint catalysts must be tested on a per gram of catalyst basis (or constant volume basis); however, this measure of activity provides little insight into the activity of catalytic sites on the various catalysts. To compare the relative activity of each catalyst on the basis of its turnover frequencies, the CO adsorption capacity of each catalyst was determined. The third column in Table 2 summarizes the adsorption capacity of each catalyst expressed in terms of moles of CO adsorbed to the total moles of platinum. This ratio typically provides an estimate of the platinum dispersion and particle size; however, the platinum particles in the L and Y zeolites may limit acces-

TABLE 2

Catalyst Activity at 420°C

| Catalyst[a] | Relative activity per gram catalyst[b] | CO chemisorption[c] (moles CO adsorbed/ mole total Pt) | Turnover Frequency[d] | |
|---|---|---|---|---|
| | | | Benzene | MCP(s)[e] |
| Pt/K L | 100 | 0.49 | 1.44 | 0.70 |
| Pt/K Y | 18 | 0.49 | 0.141 | 0.21 |
| Pt/Na Y | 16 | 0.34 | 0.155 | 0.27 |
| Pt/K-$Al_2O_3$ | 5 | 0.55 | 0.051 | 0.12 |
| Pt/$SiO_2$ | 3 | 0.22 | 0.032 | 0.084 |

[a] Each catalyst contains 1.0 wt% Pt.

[b] Relative Activity per gram of catalyst—the space velocity required by a catalyst to attain a given *n*-hexane conversion divided by the space velocity required by a reference catalyst to attain the same *n*-hexane conversion. The Pt/K L-zeolite catalyst was designated as the reference catalyst. Evaluated at 10% *n*-hexane conversion.

$$\text{Relative Activity} = \left[\frac{\text{WHSV}_{\text{catalyst}}}{\text{WHSV}_{\text{reference}}}\right]_{\text{conv}} \times 100.$$

[c] CO chemisorption—moles of CO adsorbed at room temperature per mole of total platinum.

[d] Molecules product/second/atoms surface Pt (assumes a CO-to-Pt ratio of one).

[e] MCP(s)—sum of methylcyclopentane, 2-methylpentane, and 3-methylpentane, i.e., turnover frequency of one–five-ring closure.

sibility to all sites when the particles fill the entire pore. Consequently, calculations based on CO chemisorption overestimate platinum particle size and underestimate metal dispersion. Based on measurements reported by others (*13*) and by us (*14*), hydrogen chemisorption values are about a factor of three higher than CO chemisorption for L-zeolite catalysts.

Carbon monoxide chemisorption, however, does provide a relative measure of the number of adsorption sites for CO. The Pt/K L and Pt/K Y had the same ratio of CO adsorption sites to the total amount of platinum, 0.49. Assuming one CO chemisorption site corresponds to an active site for one–five- and one–six-ring closures, turnover frequencies for these reactions can be compared. Table 2 summarizes the turnover frequencies for the formation of benzene and for one–five-ring closure (sum of methycyclopentane, 2-methylpentane, and 3-methylpentane) at 420°C. The catalysts generally rank in the same order as they did on a per gram of catalyst basis with Pt/K L the most active and Pt/$SiO_2$ the least active. On a turnover frequency basis, the Pt/Na Y catalyst is more active than the Pt/K Y, because it exhibited nearly the same activity per gram of catalyst, but the Pt/Na Y had lower CO adsorption capacity. The Pt/K L catalyst exhibits a higher turnover frequency for one–six-ring closure than for

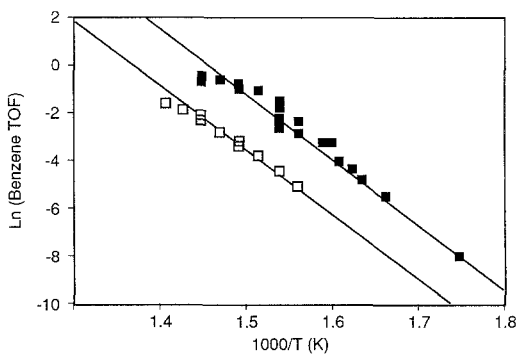


FIG. 8. An Arrhenius fit of the temperature dependence observed for benzene formation (one–six-ring closure) of the Pt/K L (■) and Pt/K Y (□) catalysts in terms of the turnover frequency (TOF).

one–five-ring closure, whereas the reverse is true for all the other catalysts.

*Apparent Activation Energies.* The apparent activation energies for one–six- and one–five-ring closure were determined for the Pt/K L and Pt/K Y catalysts based on turnover frequencies. The space velocity was chosen such that the *n*-hexane conversions would be less than 15% at all temperatures investigated. Using the assumption of differential conversion over this conversion range and assuming that the rates of back-reactions could be neglected, the rate of benzene production and the rate of one–five-ring closure (sum of the rates of methylcyclopentane, 2-methylpentane, and 3-methylpentane) were calculated over temperature ranges of 330 to 420°C for the Pt/K L catalyst and 370 to 430°C for the Pt/K Y catalyst. Rates were calculated on a turnover frequency (TOF) basis (molecules produced/Pt surface site/second) with the number of platinum surface sites determined by CO chemisorption; refer to Table 2. The observed TOFs were fitted to an Arrhenius-type temperature dependence, and Figs. 8 and 9 show these fits for the one–six- and one–five-ring closures, respectively. Both figures show the measured experimental values and a least-squares fit of these values. Table 3 summarizes the apparent activation energies for both catalysts and both ring closure reactions. Both catalysts have essentially the same apparent activation energy for each cyclization reaction, 54 kcal/mol for one–six-ring closure and 39 kcal/mole for one–five-ring closure. As shown in Figs. 8 and 9, the rate of one–six-ring closure dominates at high temperature, whereas at low temperature, one–five-ring closure exceeds the rate of one–six-ring closure. As shown in Table 3, differences in the turnover frequencies are associated with the Arrhenius preexponential terms. The similarity in apparent activation energies for both ring closure reactions on Pt/KL and Pt/KY suggests the mechanisms for formation of these products are the same on both catalysts.

TABLE 3

Kinetic Parameters[a]

| Catalyst | Benzene formation | | Methylcyclopentane formation | |
|---|---|---|---|---|
| | $\ln(k_0)$[b] | Activation energy (kcal/mole) | $\ln(k_0)$[b] | Activation energy (kcal/mole) |
| Pt/K L | 37 | 54 | 25 | 39 |
| Pt/K Y | 31 | 54 | 21 | 39 |

[a] The temperature dependence was fitted to an Arrhenius equation: $\ln(\mathrm{TOF}) = \ln(k_0 C_0) - E_a/R^*(1/T)$; where TOF is the turnover frequency, $k_0$ is the Arrhenius preexponentional factor (which includes any entropy effect), $C_0$ is the moles of *n*-hexane per mole of platinum site, $E_a$ is the activation energy, $R$ is the universal gas constant, and $T$ is the temperature in Kelvin.

[b] $k_0$ has units of inverse seconds.

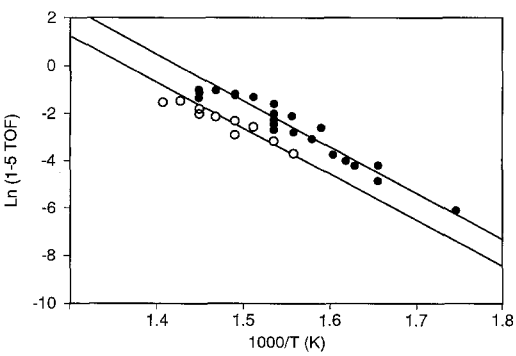


FIG. 9. An Arrhenius fit of the temperature dependence observed for methylcyclopentane formation (one–five-ring closure) of the Pt/K L (●) and Pt/K Y (○) catalysts in terms of the turnover frequency (TOF).

*Relative catalyst activities at high total hexane conversion.* In the previous discussion, the increased activity (TOF or per gram of catalyst) and the improved benzene selectivity of the Pt/K L-zeolite catalyst compared with the Pt/K Y-zeolite catalyst have been considered independently. In Fig. 7 and Table 2, the relative activities were compared at differential conversions; the Pt/K L-zeolite catalyst had a relative

activity of 100, and the Pt/K Y-zeolite catalyst had a relative activity of 18. For example, if at low conversion 100 moles of *n*-hexane were converted over the Pt/K L-zeolite catalyst at 420°C, the converted product would contain 57 mol of benzene and 39 mol of hexane isomers (methylcyclopentane, 2-methylpentane, and 3-methylpentane) and 4 wt% $C_1$–$C_5$ light gas. On the other hand, if *n*-hexane was reacted over the Pt/K Y-zeolite catalyst at the same conditions with an equivalent mass of catalyst, the converted product would contain 6 mol of benzene and 10 mol of hexane isomers and 2 wt% $C_1$–$C_5$ light gas. The advantages of the Pt/K L-zeolite catalyst are, however, accentuated at high conversion. At high conversion, 2-methylpentane and 3-methylpentane are the predominant hexane isomers which must be converted to benzene. Before the *iso*-hexanes can be converted to benzene, they must first isomerize, through methylcyclopentane, to *n*-hexane; Fig. 1. The rate of benzene formation from 2-methylpentane and 3-methylpentane is, therefore, slower at high conversion since the isomerization of hexane isomers to *n*-hexane proceeds with a lower TOF (see tables) and isomerization must preceed aromatization.

Figure 10 compares the total $C_6$ conversion as a function of inverse space velocity.

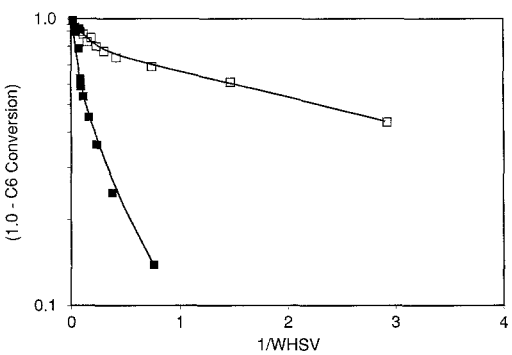


FIG. 10. Comparison of Pt/K L-zeolite (■) and Pt/K Y-zeolite (□) catalyst activities for total $C_6$ conversion. Conditions are 420°C and a molar feed ratio of $H_2$/*n*-hexane of 7.8.

For the Pt/K Y-zeolite catalyst, for example, there are two regions: one at low conversion, which is predominantly the conversion of *n*-hexane to methylcyclopentane and benzene, and a second region at high conversion (evident as a change in the slope of the curve), which is dominated by the back reactions of the 2-methylpentane and 3-methylpentane. If the catalyst activities are compared at high total $C_6$ conversion (>70%), the Pt/K Y-zeolite catalyst has a relative activity (per gram of catalyst) of 5 compared with 100 for the Pt/K L-zeolite catalyst. Catalyst activities at high conversion more nearly represent differences at practical conversion levels. The activity of the Pt/K L-zeolite catalyst increases from 6 times the activity of the Pt/K Y-zeolite catalyst at low conversion (*n*-hexane) to 20 times the activity at high total $C_6$ conversion. The increase in relative activity of the Pt/K L-zeolite catalyst at high conversion results from a combination of the higher TOFs for one–six- and one–five-ring closure and the higher selectivity for one–six-ring closure.

## DISCUSSION

Since both the reaction pathway and activation energies for Pt/KL and Pt/KY are identical, it appears likely that the observed differences in benzene selectivities and TOFs result from, predominantly, geometric influences. In the following section, our data are interpreted with respect to the molecular die hypothesis and the confinement model.

### *Molecular Die Hypothesis*

As previously discussed, the molecular die hypothesis suggests that the high aromatic selectivity for Pt/K L results from terminal adsorption of *n*-hexane (*6, 7*). According to this hypothesis, the degree of terminal adsorption is estimated by determining the terminal cracking index (TCI), which is defined as the molar ratio of pentanes to butanes in the gaseous products. A high value for the TCI suggests that there is pref-

TABLE 4

Terminal Cracking Index at 420°C

| Catalyst[a] | Terminal cracking index[b] | Benzene selectivity[c] |
|---|---|---|
| Pt/K L | 1.8 | 0.92 |
| Pt/K Y | 3.1 | 0.88 |
| Pt/NaY | 1.5 | 0.84 |
| Pt/K-$Al_2O_3$ | 1.7 | 0.86 |
| $Pt/SiO_2$ | 1.0 | 0.65 |

[a] Each catalyst contains 1.0 wt% Pt.

[b] Terminal cracking index is defined as the mole ratio of pentanes to butanes (*6*). TCI were extrapolated to 0% *n*-hexane conversion.

[c] Selectivity is defined as the wt% benzene/(wt% benzene + wt% $C_2$–$C_5$ gas) (*2*). Selectivities were extrapolated to 0% *n*-hexane conversion.

erential adsorption of the terminal carbon of *n*-hexane. With high terminal adsorption, the selectivity for one–six-ring closure is suggested to be enhanced. The terminal cracking indices for these five catalysts extrapolated to 0% *n*-hexane conversion are given in Table 4. The $Pt/SiO_2$ catalyst exhibits a TCI of 1.0; a TCI near 1.0 for $Pt/SiO_2$ is consistent with previous studies (*2, 6, 7*). Both the Pt/K L-zeolite and Pt/K Y-zeolite catalysts have terminal cracking indices larger than 1.0 suggesting a preference for terminal adsorption. Note, however, that the TCI for Pt/K $Al_2O_3$ is 1.7 which is nearly identical to the value for the Pt/L zeolite catalyst.

Also given in Table 4 are the benzene selectivities (defined as the wt% benzene/[wt% benzene + wt% $C_2$–$C_5$ gas] (*2, 6, 7*)) extrapolated to 0% *n*-hexane conversion. The benzene selectivities calculated for TCI in Table 4 do not include the formation of $CH_4$ (*2, 6, 7*). From Table 4, the Pt/K $Al_2O_3$ catalyst displays a higher TCI and benzene selectivity than Pt/Na Y; however, the Pt/K $Al_2O_3$ would not be expected to favor terminal adsorption of *n*-hexane relative to Pt/Na Y. In addition, the TCI of 1.7 for Pt/K $Al_2O_3$ is also nearly identical to Pt/K L. Furthermore, it is not known why the TCI of Pt/K Y is very high, 3.1, compared with the other catalysts.

Since $CH_4$ is an important by-product in the aromatization of hexane, it should not be excluded in the determination of benzene selectivities. The benzene selectivities as calculated for the TCI are similar for each catalyst, except $Pt/SiO_2$, ranging from 0.84 to 0.92. Benzene selectivities, however, which include the formation of $CH_4$, i.e., ultimate benzene selectivity and given in Table 1, readily differentiate each catalyst's benzene selectivity, and do not correlate with the terminal cracking index. We conclude, therefore, that the hypothesis of terminal adsorption does not adequately explain the enhanced aromatic selectivity of the Pt/K L catalyst and does not provide a satisfactory basis for rationalization of the increased reaction rate for Pt/K L.

*Confinement (Configuration) Model*

According to the confinement model, nonbinding interactions of *n*-hexane with the zeolite lead to adsorption as a pseudocycle. Based on molecular modeling calculations, the L-zeolite pore size is optimum for preorganization of *n*-hexane as a six-ring pseudo-cycle which resembles the transition state in the formation of benzene (*8*).

Although in Y zeolite the dimensions of the supercage are not optimum (too large) for the six-ring pseudo-cycle, cyclic adsorption of hexane in Pt/Na Y and Pt K Y lead to enhanced benzene selectivity and rate; Tables 1 and 2, respectively, relative to $Pt/SiO_2$ or Pt/K $Al_2O_3$, where nonbinding interactions are minimized. The benzene activity and selectivity is further increased in Pt/K L where pore size results in hexane adsorption which more closely resembles the transition state for benzene formation.

The confinement model is also consistent with the increased activity of one–five-ring closure, e.g., methylcyclopentane, 2-methylpentane, and 3-methylpentane, in Pt/K L relative to Pt/K Y. The rate of methylcyclopentane is expected to be increased when the adsorption of hexane leads to the preor-

ganization of a five-ring pseudo-cycle. Although neither L nor Y zeolite is the optimum pore size for the five-ring pseudo-cycle, the smaller pore L zeolite more closely matches the steric requirements for a five-ring transition state. Despite the lower one–five-ring closure selectivity for L zeolite, the TOF for one–five-ring closure in Pt/K L is 3.3 times higher than Pt/K Y. We conclude that our data are consistant with the confinement model and that nonbinding interactions of the reactant adsorbate with the zeolite walls strongly influence the selectivity and activity of the catalyst.

## SUMMARY

The reaction pathways for *n*-hexane over Pt/K L and Pt/K Y catalysts are similar, but the catalysts differ in their selectivity for one–six- and one–five-ring closure. The selectivity for one–six-ring closure on the Pt/K L-zeolite catalyst was two to three times higher than for other catalysts; furthermore, the selectivity for one–six-ring closure increased at high *n*-hexane conversions. In addition, the Pt/K L-zeolite catalyst was more active than the other catalysts. The turnover frequency for Pt/K L compared with Pt/K Y was 10 times higher for one–six-ring closure and 3.3 times higher for one–five-ring closure. Although the catalysts have different activities, they have the same apparent activation energies: 54 kcal/mol for one–six-ring closure and 39 kcal/mol for one–five-ring closure.

The increased selectivity and activity for one–six-ring closure observed for the L-zeolite catalyst is consistent with an influence of the zeolite geometry on the transition state, i.e., the confinement (conformation) model (*8*). In L zeolite, adsorption forces between *n*-hexane and the zeolite channel may lead to preorganization of the transition state for direct benzene formation. In addition, this model can account for the increased turnover frequency of other reactions, e.g., the formation of methylcyclopentane.

## REFERENCES

1. Bernard, J. R. Nury, J., U.S. Patent 4,104,320 to Elf France (1978).
2. Fung, S. C., Tauster, S. J., and Koo, J. Y., European Patent 0142352 to Exxon (1984).
3. Law, D. V., Tamm, P. W., and Detz, C. M., *Energy Prog.* **7,** 215 (1987).
4. Tamm, P. W., Mohr, D. H., and Wilson, C. R., in "Catalysis 1987" (Stud. Surf. J. W. Ward, Ed.), Vol. 38, pp. 335–353. Studies in Surface Science and Catalysis, Elsevier, Amsterdam/New York, 1988.
5. Bernard, J. R. *in* "Proceedings, 5th International Conference on Zeolites" (L. V. C. Rees, Ed.), pp. 686–695. Wiley, New York, 1980.
6. Tauster, S. J., and Steger, J. J., *Mater. Res. Soc. Symp. Proc.* **111,** 419 (1988).
7. Tauster, S. J., and Steger, J. J., *J. Catal.* **125,** 387 (1990).
8. Derouane, E. G., and Vanderveken, D. J., *Appl. Catal.* **45,** L15 (1988).
9. Besoukhanova, C., Guidot, J., Barthomeuf, D., Breysse, M., and Bernard, J., *J. Chem. Soc., Faraday Trans. 1* **77,** 1595 (1981).
10. Moreti, G., and Sachtler, W. M. H., *J. Catal.* **116,** 35 (1989).
11. Freel, J., *J. Catal.* **25,** 139 (1972).
12. Bhore, N. A., Klein, M. T., and Bischoff, K. B., *Ind. Eng. Chem. Res.* **29,** 313 (1990).
13. Larsen, G., and Haller, G. L., *Catal. Lett.* **3,** 103 (1989).
14. Vaarkamp, M., Grondelle, J. V., Miller, J. T., Sajkowski, D. J., Modica, F. S., Lane, G. S., Gates, B. C., Koningsberger, D. C., *Catal. Lett.* **6,** 369 (1990).